Optical gain in single tensile-strained germanium photonic wire

M. de Kersauson,[1] M. El Kurdi,[1,*] S. David,[1] X. Checoury,[1] G. Fishman,[1] S. Sauvage,[1] R. Jakomin,[2] G. Beaudoin,[2] I. Sagnes,[2] and P. Boucaud[1]

[1]*Institut d'Electronique Fondamentale, CNRS - Univ. Paris-Sud 11, Bâtiment 220, F-91405 Orsay, France*

[2]*Laboratoire de Photonique et de Nanostructures, CNRS - UPR 20, Route de Nozay 91460 Marcoussis, France*

**moustafa.el-kurdi@ief.u-psud.fr*

http://pages.ief.u-psud.fr/QDgroup

Abstract: We have investigated the optical properties of tensile-strained germanium photonic wires. The photonic wires patterned by electron beam lithography (50 μm long, 1 μm wide and 500 nm thick) are obtained by growing a *n*-doped germanium film on a GaAs substrate. Tensile strain is transferred in the germanium layer using a Si_3N_4 stressor. Tensile strain around 0.4% achieved by the technique corresponds to an optical recombination of tensile-strained germanium involving light hole band around 1690 nm at room temperature. We show that the waveguided emission associated with a *single* tensile-strained germanium wire increases superlinearly as a function of the illuminated length. A 20% decrease of the spectral broadening is observed as the pump intensity is increased. All these features are signatures of optical gain. A 80 cm^{-1} modal optical gain is derived from the variable strip length method. This value is accounted for by the calculated gain material value using a 30 band $\mathbf{k}\cdot\mathbf{p}$ formalism. These germanium wires represent potential building blocks for integration of nanoscale optical sources on silicon.

OCIS codes: (230.0250) Optoelectronics; (300.6470) Spectroscopy, semiconductors; (310.6860) Thin films, optical properties; (250.4480) Optical amplifiers.

References and links

1. J. Liu, X. Sun, L. C. Kimerling, and J. Michel, "Direct-gap optical gain of Ge on Si at room temperature," Opt. Lett. **34**, 1738–1740 (2009).
2. J. Liu, X. Sun, R. Camacho-Aguilera, L. C. Kimerling, and J. Michel, "Ge-on-Si laser operating at room temperature," Opt. Lett. **35**, 679–681 (2010).
3. D. Liang and J. E. Bowers, "Recent progress in lasers on silicon," Nat. Photonics **4**, 511–517 (2010).
4. J. Menendez and J. Kouvetakis, "Type-I $Ge/Ge_{1-x-y}Si_xSn_y$ strained-layer heterostructures with a direct Ge bandgap," Appl. Phys. Lett. **85**, 1175–1177 (2004).
5. Y. Bai, K. E. Lee, C. Cheng, M. L. Lee, and E. A. Fitzgerald, "Growth of highly tensile-strained Ge on relaxed $In_xGa_{1-x}As$ by metal-organic chemical vapor deposition," J. Appl. Phys. **104**, 084518 (2008).
6. Y. Huo, H. Lin, R. Chen, M. Makarova, Y. Rong, M. Li, T. I. Kamins, J. Vuckovic, and J. S. Harris, "Strong enhancement of direct transition photoluminescence with highly tensile-strained Ge grown by molecular beam epitaxy," Appl. Phys. Lett. **98**, 011111 (2011).

#147489 - $15.00 USD Received 12 May 2011; revised 22 Jul 2011; accepted 1 Aug 2011; published 29 Aug 2011

7. R. Jakomin, M. de Kersauson, M. E. Kurdi, L. Largeau, O. Mauguin, G. Beaudoin, S. Sauvage, R. Ossikovski, G. Ndong, M. Chaigneau, I. Sagnes, and P. Boucaud, "High quality tensile-strained n-doped germanium thin films grown on InGaAs buffer layers by metal-organic chemical vapor deposition," Appl. Phys. Lett. **98**, 091901 (2011).
8. M. El Kurdi, H. Bertin, E. Martincic, M. de Kersauson, G. Fishman, S. Sauvage, A. Bosseboeuf, and P. Boucaud, "Control of direct band gap emission of bulk germanium by mechanical tensile strain," Appl. Phys. Lett. **96**, 041909 (2010).
9. T.-H. Cheng, K.-L. Peng, C.-Y. Ko, C.-Y. Chen, H.-S. Lan, Y.-R. Wu, C. W. Liu, and H.-H. Tseng, "Strain-enhanced photoluminescence from Ge direct transition," Appl. Phys. Lett. **96**, 211108 (2010).
10. R. S. Jacobsen, K. N. Andersen, P. I. Borel, J. Fage-Pedersen, L. H. Frandsen, O. Hansen, M. Kristensen, A. V. Lavrinenko, G. Moulin, H. Ou, C. Peucheret, B. Zsigri, and A. Bjarklev, "Strained silicon as a new electro-optic material," Nature **441**, 199–202 (2006).
11. R. Jakomin, G. Beaudoin, N. Gogneau, B. Lamare, L. Largeau, O. Mauguin, and I. Sagnes, "p and n-type germanium layers grown using iso-butyl germane in a III-V metal-organic vapor phase epitaxy reactor," Thin Solid Films **519**, 4186–4191 (2011).
12. M. de Kersauson, R. Jakomin, M. El Kurdi, G. Beaudoin, N. Zerounian, F. Aniel, S. Sauvage, I. Sagnes, and P. Boucaud, "Direct and indirect band gap room temperature electroluminescence of Ge diodes," J. Appl. Phys. **108**, 023105 (2010).
13. J. Liu, X. Sun, D. Pan, X. Wang, L. C. Kimerling, T. L. Koch, and J. Michel, "Tensile-strained, n-type Ge as a gain medium for monolithic laser integration on Si," Opt. Express **15**, 11272–11277 (2007).
14. M. El Kurdi, T. Kociniewski, T.-P. Ngo, J. Boulmer, D. Debarre, P. Boucaud, J. F. Damlencourt, O. Kermarrec, and D. Bensahel, "Enhanced photoluminescence of heavily n-doped germanium," Appl. Phys. Lett. **94**, 191107 (2009).
15. V. Yam, V. Le Thanh, Y. Zheng, P. Boucaud, and D. Bouchier, "Photoluminescence study of a bimodal size distribution of Ge/Si(001) quantum dots," Phys. Rev. B **63**, 033313 (2001).
16. J. O'Gorman, S. L. Chuang, and A. F. J. Levi, "Carrier pinning by mode fluctuations in laser diodes," Appl. Phys. Lett. **62**, 1454–1456 (1993).
17. J. R. Haynes, "New radiation resulting from recombination of holes and electrons in germanium," Phys. Rev. **98**, 1866–1868 (1955).
18. K. L. Shaklee and R. F. Leheny, "Direct determination of optical gain in semiconductor crystals," Appl. Phys. Lett. **18**, 475–477 (1971).
19. M. D. McGehee, R. Gupta, S. Veenstra, E. K. Miller, M. A. Díaz-García, and A. J. Heeger, "Amplified spontaneous emission from photopumped films of a conjugated polymer," Phys. Rev. B **58**, 7035–7039 (1998).
20. X. Sun, J. Liu, L. C. Kimerling, and J. Michel, "Room-temperature direct bandgap electroluminesence from Ge-on-Si light-emitting diodes," Opt. Lett. **34**, 1198–1200 (2009).
21. S.-L. Cheng, J. Lu, G. Shambat, H.-Y. Yu, K. Saraswat, J. Vuckovic, and Y. Nishi, "Room temperature 1.6 μm electroluminescence from Ge light emitting diode on Si substrate," Opt. Express **17**, 10019–10024 (2009).
22. W. Klingenstein and H. Schweizer, "Direct gap recombination in germanium at high excitation level and low temperature," Solid-State Electron. **21**, 1371–1374 (1978).
23. R. Conradt and J. Aengenheister, "Minority carrier lifetime in highly doped Ge," Solid State Commun. **10**, 321–323 (1972).
24. M. El Kurdi, G. Fishman, S. Sauvage, and P. Boucaud, "Band structure and optical gain of tensile-strained germanium based on a 30 band $\mathbf{k}\cdot\mathbf{p}$ formalism," J. Appl. Phys. **107**, 013710 (2010).
25. M. El Kurdi, S. Sauvage, G. Fishman, and P. Boucaud, "Band-edge alignment of SiGe/Si quantum wells and SiGe/Si self-assembled islands," Phys. Rev. B **73**, 195327 (2006).
26. S.-W. Chang and S. L. Chuang, "Theory of optical gain of Ge-$Si_xGe_ySn_{1-x-y}$ quantum-well lasers," IEEE J. Quantum Electron. **43**, 249–256 (2007).
27. L. Allen and G. I. Peters, "Amplified spontaneous emission and external signal amplification in an inverted medium," Phys. Rev. A **8**, 2031–2047 (1973).
28. M. El Kurdi, S. David, X. Checoury, G. Fishman, P. Boucaud, O. Kermarrec, D. Bensahel, and B. Ghyselen, "Two-dimensional photonic crystals with pure germanium-on-insulator," Opt. Commun. **281**, 846–850 (2008).
29. T.-P. Ngo, M. El Kurdi, X. Checoury, P. Boucaud, J. F. Damlencourt, O. Kermarrec, and D. Bensahel, "Two-dimensional photonic crystals with germanium on insulator obtained by a condensation method," Appl. Phys. Lett. **93**, 241112 (2008).
30. J. C. Johnson, H.-J. Choi, K. P. Knutsen, R. D. Schaller, P. Yang, and R. J. Saykally, "Single gallium nitride nanowire lasers," Nat. Mater. **1**, 106–110 (2002).
31. X. Duan, Y. Huang, R. Agarwal, and C. M. Lieber, "Single-nanowire electrically driven lasers." Nature **421**, 241 (2003).
32. M. A. Zimmler, F. Capasso, S. Moller, and C. Ronning, "Optically pumped nanowire lasers: invited review," Semicond. Sci. Technol. **25**, 024001 (2010).

#147489 - $15.00 USD Received 12 May 2011; revised 22 Jul 2011; accepted 1 Aug 2011; published 29 Aug 2011

1. Introduction

Optical gain has been recently observed by pump-probe measurement in *n*-doped tensile-strained germanium at room temperature [1]. This observation was shortly followed by the demonstration of a germanium laser under pulsed optical pumping, establishing a new paradigm for the integration of an efficient optical source on a silicon platform [2,3]. In both experiments, germanium was directly grown on silicon and a tensile strain around 0.25% was obtained due to the difference of thermal dilatation coefficients between germanium and silicon. Several alternative approaches exist to transfer a tensile strain in germanium films. Growth on GeSn layers [4] or relaxed InGaAs buffer layers [5–7] have been successfully demonstrated as well as the application of an external mechanical stress [8,9]. The possibility to achieve a large tensile strain in germanium is of tremendous importance as the optical gain magnitude directly depends on this parameter. The tensile strain decreases the energy difference between the *L* and Γ valley, from 140 meV for unstrained germanium down to 0 for 1.9% tensile-strained germanium, i.e. corresponding to a direct band gap material, thus enhancing the population and carrier recombination at the Brillouin zone center. The tensile strain also lifts the degeneracy of the valence band, pushing the light hole band at higher energy. Another possibility to impose a tensile stress is to use silicon nitride layers as external stressors. This local strain engineering method was pioneered by the microelectronics industry to enhance the mobility properties of transistors. In the latter case, the typical size of the strained channel regions is in the tens of nanometer range, i.e. much smaller than the one required for optical experiments with strained layers. It was later applied to silicon to break the crystal symmetry and to fabricate an active electro-optic material [10].

In this letter, we show that Si_3N_4 straining layers can be used to fabricate optically active tensile-strained germanium photonic wires. We study the room temperature direct band gap optical recombination in the germanium nanowires. Optical gain is observed at room temperature under continuous wave optical pumping, as evidenced by the superlinear increase of the emission as a function of the illuminated length and spectral narrowing as the pump power is increased. A net optical modal gain of ~ 80 cm^{-1} is measured from the experiments. This value is found in agreement with the calculated gain material value using a 30 band $\mathbf{k}\cdot\mathbf{p}$ formalism. The demonstration of optical gain with germanium photonic wires opens new perspectives for future integration of efficient nanoscale optical sources on silicon.

2. Sample Fabrication

The germanium layers were grown on GaAs substrate by metal-organic chemical vapor deposition (MOCVD) [11,12]. The interest of the growth on GaAs is three-fold: as germanium and gallium arsenide are lattice-matched, high quality germanium films can be obtained without the presence of misfit dislocations at the interface as it occurs when growing germanium on silicon. The large difference of refractive index between germanium and GaAs leads to the formation of an optical waveguide for propagation in the layer plane. Finally, the difference of chemical etching properties between Ge and GaAs is also used for underetching and transferring more efficiently stress in the germanium layer. The MOCVD allows to simultaneously grow germanium films with high optical quality and strong *n*-type doping as large as 3 x 10^{19} cm^{-3}. The *n*-type doping of Ge is of high importance in order to increase the radiative recombination of the direct gap and the optical gain [13,14]. The Si_3N_4 straining layers containing a fraction of hydrogen, i.e. corresponding to a SiN_xH_y composition, were deposited by plasma-enhanced chemical vapor deposition. Depending on the growth conditions, compressively-strained or tensile-strained layers can be obtained. The stress amplitude can be increased or reversed by subsequent thermal annealing. In our experiments, a 500 nm thick *compressively*-strained Si_3N_4 layer was deposited at 300°C using low frequency plasma-enhanced chemical vapor deposition. Stress

#147489 - $15.00 USD Received 12 May 2011; revised 22 Jul 2011; accepted 1 Aug 2011; published 29 Aug 2011

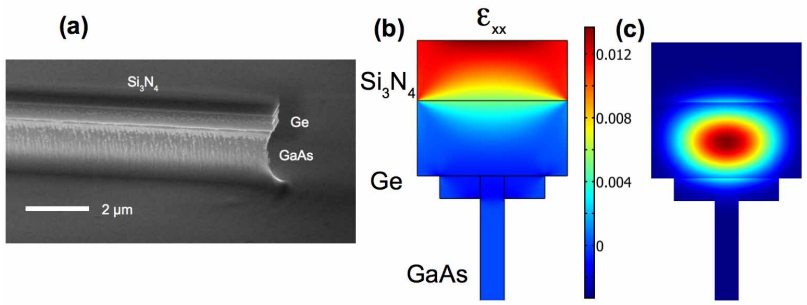

Fig. 1. (a) Scanning electron microscope image of a fabricated tensile-strained germanium wire. (b) Calculated strain field (ε_{xx}) in the layer plane perpendicular to the wire direction. The top of the Ge wire is tensile-strained (0.6%). The bottom of the wire close to GaAs is compressively-strained. The color bar indicates the magnitude of the strain. (c) Calculated two-dimensional mode profile in TM polarization.

as high as 1.3 GPa can be achieved by this technique. The nanowire patterns were defined by electronic lithography. The typical sizes of the wires that were optically investigated are 50 μm length, 1 μm width and 500 nm thickness. The nitride layer was then etched by reactive ion etching followed by the etching of germanium down to the GaAs interface by inductively coupled plasma etching. As the nitride layer is free to move once its flanks have been etched, a uniaxial tensile strain perpendicular to the wire long axis is transferred into the germanium film. In order to enhance the transferred strain, the GaAs substrate below the wire was then underetched by inductively plasma etching using a rather isotropic etching recipe. The Si_3N_4 layer is used as a hard mask for this step. The whole process can obviously be down-scaled in order to obtain smaller wires. Figure 1(a) shows a scanning electron microscope image of the fabricated structure. Figure 1(b) shows the strain profile ε_{xx} in the wire calculated using a finite element method. The transferred strain is inhomogeneous, going from a tensile strain on top of the wire to a compressive strain at the bottom of the wire close to GaAs. A uniaxial strain of 0.6% along [110] is calculated at the top of the wire. More than half of the wire thickness is tensily strained. Since the Ge wire edges are free to bend while it is clamped at the center to the GaAs, the elongation in the vertical direction is different from the one encountered for a biaxial deformation. Figure 1(c) shows the calculated two-dimensional mode profile in TM polarization.

3. Optical Measurements

All optical experiments were carried out at room temperature. The germanium wires were optically pumped using a cw 532 nm laser and the luminescence was collected from the surface [15]. The advantage of a 532 nm optical pump is that it is absorbed in the upper part of germanium with an absorption coefficient of 5×10^5 cm^{-1} where the tensile strain is maximum. The Si_3N_4 straining layer acts as an antireflection coating for the optical pump. It also limits the surface recombination by passivation but its main role is to transfer a tensile stress in the germanium wire. A combination of cylindrical lens and microscope objective was used in order to homogeneously illuminate the wires. The emitted light was detected with a liquid-nitrogen cooled germanium photodetector or a PbS detector with a lower sensitvity but a broader spectral range for detection. Figure 2(a) shows a far-field image of a luminescent wire obtained with a room temperature InGaAs camera. The photoluminescence signal is collected from the entire wire length. The luminescence radiates from all parts of the wire but with a clear enhanced scattering at the ends of the wire. This enhancement suggests that a significant part of the lumi-

#147489 - $15.00 USD Received 12 May 2011; revised 22 Jul 2011; accepted 1 Aug 2011; published 29 Aug 2011

nescence is waveguided rather than directly radiated. Although we do not collect the emission along the wire axis, the end of the wire acts as an outcoupler that redirects the emission. The emission amplitude at the facet is around 5 times larger than the one at the waveguide center. We note that the roughness of the waveguide also contributes to scattering of the waveguided light. The emission along the wire axis is uniform indicating that the optical pumping is rather homogeneous over the total wire length. Figure 2(b) shows the spectral dependence of the collected emission for a 20 mW pump power corresponding to a 6 kW.cm^{-2} pump intensity. A broad luminescence band peaked at 1560 nm is observed and is associated with the direct band gap recombination of unstrained germanium. The strong doping of the layer contributes to the broadening. A narrow luminescence band maximum at 1680 nm is superimposed on top of this broad luminescence and as explained below is associated with the direct band gap optical recombination of tensile-strained germanium. Figure 2(b) also shows the photoluminescence of the germanium wire after removal of the Si_3N_4 straining layer by fluorhydric acid. Only the broad luminescence of the unstrained germanium is observed in this case, emphasizing the critical role of the nitride layer in our experiments for stress transfer. Note that as the photoluminescence is still observed after removal of the nitride layer, the quenching of the resonance at 1680 nm is not due to a lack of passivation but to the absence of stress. The spectral position of the narrow luminescence varies from wires to wires and is dependent on the effective strain magnitude that depends on the processing. An optical recombination around 1680 nm corresponds to an equivalent 0.4% biaxial strain if we consider that the light hole band is involved in the recombination [8]. This value is close to the one calculated in Fig. 1(b), the equivalent biaxial strain being less than a factor of two smaller than the uniaxial strain. Recombination involving light holes is expected to be more intense in waveguided emission as compared to surface emission because of the *z*-orientation of the matrix elements. As compared to the broad recombination of germanium that is directly radiated, the linewith of the strained waveguided emission is significantly reduced because of self-absorption. The propagation of the emission leads indeed to a linewidth reduction because of the presence of the absorption edge of the direct gap. This absorption edge quenches the emission at high energy where the absorption is the most pronounced [16]. This linewidth reduction by propagation was already discussed and evidenced in the first electroluminescence experiments performed on germanium diodes [17]. We have recently observed in electroluminescence measurements direct band gap emission of germanium with a 40 nm full width at half maximum [12], significantly smaller than the 1.8 k_BT photoluminescence broadening expected for a direct band gap semicondutor. The reduced linewidth for guided light in weak excitation regime does not conclusively prove that optical gain is present in the nanowires.

We have studied the dependence of the optical emission as a function of the illuminated length following the variable strip length method [18, 19]. The principle consists in optically pumping a sample with a stripe of variable length and detecting the intensity of the light out of the end of the stripe. In our experiments, the stripe is laterally defined by the Ge nanowire and the pumping length is varied along its main axis. A fraction of the light emitted from the facet is collected and filtered from the rest of the wire using a pinhole in a confocal geometry. Note that we do not collect the waveguided light along the wire axis but rather the fraction of it scattered perpendicular to the wire axis. Figure 3(a) shows the spectral dependence of the emission collected from the facet as a function of the illuminated length. The incident pump power is 20 mW. A background signal of non-guided emission is still present on the measurements at small illuminated lengths because of diffraction effects. In the following, this background signal was subtracted by a linear interpolation to zero length of the spectra for 10 and 20 μm illuminated length. After background subtraction (not shown), the linewidth of the emission around 1680 nm is similar to the one shown in Fig. 2(b). Depending on the wavelength, the

#147489 - $15.00 USD Received 12 May 2011; revised 22 Jul 2011; accepted 1 Aug 2011; published 29 Aug 2011

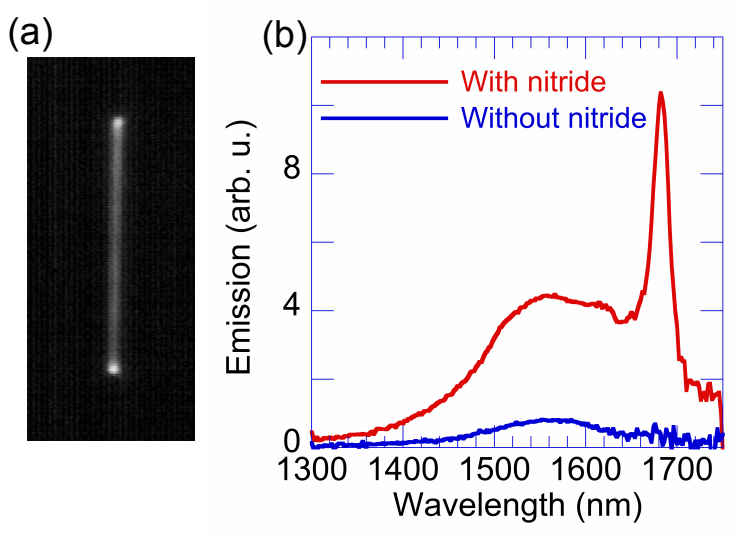

Fig. 2. (a) Room temperature photoluminescence of a germanium wire. The total length is 50 µm. Enhanced scattered emission is observed at the end of the wire. (b) Emission spectrum of a wire as measured with the nitride stressor (top curve) or after removing the nitride stressor (bottom curve).

signal amplitude exhibits a superlinear dependence or a sublinear dependence as a function of the illuminated length. Figure 3(b) shows the amplitude signal at 1684 nm where a superlinear increase is observed. If amplified spontaneous emission is present, one expects in a simple one dimensional model that the amplitude collected at the wire edge follows the following dependence : $I(\lambda, l) \propto \frac{1}{g(\lambda)}(e^{g(\lambda)l} - 1)$ where g = g_0 - α is the net optical gain with g_0 the modal gain and α the optical losses [18]. We neglect any contribution of the light reflected from the opposite facet as we did not observe any Fabry-Perot contrast on the spectra that would be expected if the reflectivity is significant. A fit to the data gives a modal gain value g $\sim$ 80 cm^{-1} $\pm$ 20 cm^{-1} (full line in Fig. 3(b)). This value is of the same order of magnitude as the one reported in Ref. [1] as measured by pump-probe measurements on tensile-strained Ge waveguides on silicon (56 cm^{-1} at 1605 nm). We emphasize that the superlinear increase observed by the variable stripe length method is different from the superlinear increase that can be observed when studying the emission as a function pump intensity for a fixed pumping length. For example, a superlinear direct gap germanium emission has been observed by electroluminescence by several authors [20, 21]. This superlinear emission is associated with the change of transition rate to the direct gap with increasing electron concentration, corresponding to an enhanced population of the zone center valley. At high carrier injection, a coupling between direct and indirect population by Auger processes can explain this enhanced zone center valley population. This coupling was introduced to explain the direct gap luminescence of germanium at low temperature in highly excited germanium [22]. In the latter case, no stimulated emission was present. Figure 3(c) shows the spectral dependence of gain deduced using the variable stripe length formula at several wavelengths. Gain is only observed in a narrow range of about 35 nm with a maximum around 1685 nm.

Variable stripe length measurements can also be performed when collecting light emitted from the whole length of the wire as seen in Fig. 2(b). The signal amplitude is significantly larger in this case. Figure 4(a) shows the spectral dependence of the collected emission from

#147489 - $15.00 USD Received 12 May 2011; revised 22 Jul 2011; accepted 1 Aug 2011; published 29 Aug 2011

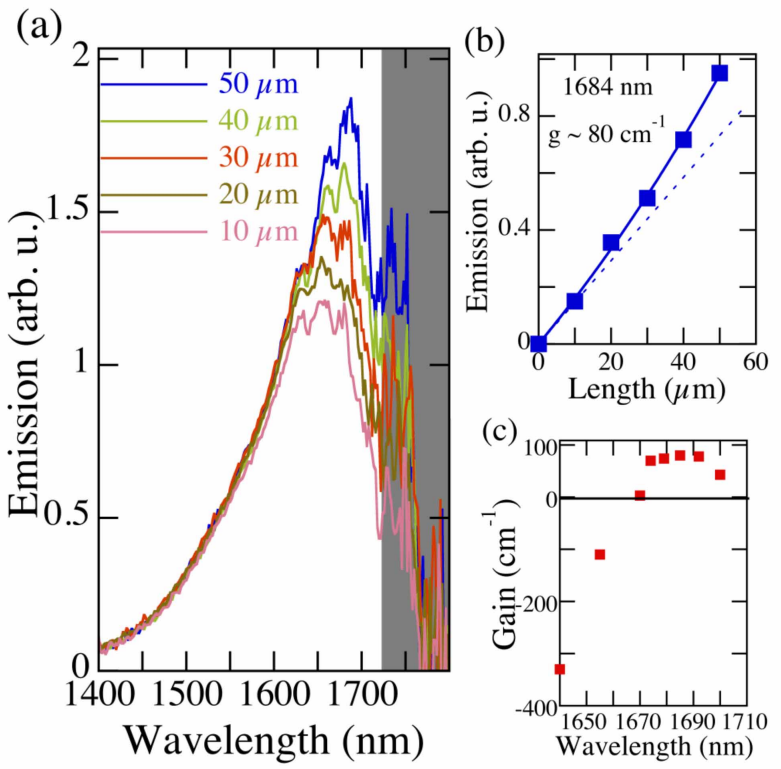

Fig. 3. (a) Emission of a photonic wire collected from one output facet as a function of the pumped length measured with a confocal set-up. The gray area corresponds to a weak detector detectivity range where the noise is significant. (b) Dependence of the amplitude emission at 1684 nm after background subtraction as a function of the pumping length. The full line is a fit according to the variable stripe length formula. The dashed line corresponding to a linear dependence of the emission is shown for clarity. (c) Spectral dependence of the optical gain. Positive gain is only observed in a narrow spectral range.

the surface as a function of the illuminated length. The wire differs from the one studied in Fig. 3 and the maximum of emission is slightly shifted. The dependence of the peak emission at 1560 nm and 1695 nm is summarized in Fig. 4(b). The 1560 nm broad emission increases linearly as a function of the illuminated length whereas the 1695 nm emission increases superlinearly. The ratio between peak and background emission thus increases significantly. No red-shift is observed indicating that thermal heating is not significant. Similar results were obtained at a lower pump power (10 mW) although with a less marked superlinear increase. When collecting light from the surface, one has to account for the collected emission coming out from the facet, the waveguided emission scattered perpendicularly to the wire axis and the non-guided spontaneous emission. The collected emission has thus the following dependence:

$$I_{coll}(\lambda,l) \propto \frac{\kappa R_{sp}}{g(\lambda)}(e^{g(\lambda)l}-1)+\frac{2R_{sp}}{g^2(\lambda)}(e^{g(\lambda)l}-1-g(\lambda)l)+R'_{sp}l \qquad (1)$$

where R_{sp} represents the waveguided emission and R'_{sp} represents the spontaneous emission collected from the surface and not channeled into a waveguide mode. The first term represents the fraction of waveguided light collected from the facet (κ is an adjustable parameter), the

#147489 - $15.00 USD Received 12 May 2011; revised 22 Jul 2011; accepted 1 Aug 2011; published 29 Aug 2011

second term the scattered waveguided emission coupled to the surface because of waveguide losses and the third term the non-waveguided spontaneous emission. In this configuration, the modes more efficiently scattered perpendicular to the wire might be different from the waveguided mode collected through the facet. The superlinear increase at 1695 nm observed in Fig. 4(b), significantly different from the linear dependence of the unstrained germanium emission, is indeed a signature of amplified spontaneous emission. The experimental data were fitted according to Eq. (1) and the gain value deduced from Fig. 3. This fit is shown as the full line in Fig. 4(b). A satisfying agreement is obtained thus confirming the presence of net optical gain. Note that an exact value of the gain is more difficult to obtain in this configuration as there are several adjustable parameters in Eq. (1). According to formula 1, we have measured a gain value of g $\sim$ 20 cm^{-1} for a 10 mW pump power and negative gain values, i.e. absorption, at pump power lower than 7 mW.

In steady-state, the photocarrier density is governed by the non-radiative and radiative recombination properties. As the doping level of germanium is high (N$_d$ = 3 x 10^{19} cm^{-3}), the non radiative Auger recombination is likely to dominate, with an effective Auger recombination time τ_A given by $\frac{1}{\tau_A} = CN_d^2$ where C is the Auger recombination coefficient (C $\sim$10^{-31}cm^{6}s^{-1}) [23] corresponding to an effective lifetime of 10 ns, as long as the photocarrier density is lower than the nominal doping. The optically injected carrier density needs to account for the carrier diffusion in the germanium layer. For a 6 kW.cm^{-2} pumping intensity, the injected carrier density in the strained layer is estimated to be around 1-2 x 10^{19} cm^{-3}. We emphasize that the wire geometry limits the carrier diffusion, allowing in turn to achieve high carrier densities. We have calculated the optical gain at room temperature that can be expected with such carrier densities following a 30 band $\mathbf{k}\cdot\mathbf{p}$ formalism [24, 25]. The calculation accounts for the strain present in the material and the free-carrier absorption due to the doping and photo-induced carriers. A material gain of 720 cm^{-1} is calculated for the recombination involving the light hole band at 1695 nm. If we account for free-carrier absorption following Ref. [26], the net optical gain is decreased to 270 cm^{-1}. This value depends obviously on the formula used to estimate the free-carrier absorption, distinct estimates being reported in the literature [13]. These gain values are given in a steady state regime and assuming a Fermi-Dirac distribution for the electron population. As mentioned above, significant deviation from this assumption can be observed at very high carrier densities [22], with an enhanced population of the high energy valleys due to electron-electron scattering. The gain values indicated above can thus be underestimated. If we consider an overlap of the waveguided TM mode of 40% with the active strained-germanium region (see the mode profile in Fig. 1(c)), and a $\sim$100 cm^{-1} absorption loss in the *n*-doped region for the remaining fraction of the mode, we deduce a modal gain value of $\sim$50 cm^{-1} in satisfying agreement with the experimental value. We note that if the recombination dynamics is governed by Auger recombination due to the high doping level, the photo-induced carrier density is expected to scale linearly with the pump intensity as well as the gain value, which is experimentally observed. Lasing is not expected in the present structure since the facet losses $\frac{1}{L}\ln(\frac{1}{R})$ where L is the wire length and R the facet reflectivity are larger than 240 cm^{-1}. The reflectivity of the facet is well below its theoretical value because of a residual roughness as observed in Fig. 1(a).

The spectral broadening of the emission was also investigated as a function of the pump power for a fixed pumping length and as a function of the pumping length for a fixed pump intensity. Figure 4(c) shows the broadening (full width at half maximum) of the emission *vs.* pump power when the wire is pumped over its total length. The broadening is measured by its full width at half maximum after subtraction of the broad background emission. One observes a decrease of the broadening from 30 nm to 24 nm at high pump power corresponding to a 20% reduction. This reduced broadening is expected when the product of gain by length

#147489 - $15.00 USD Received 12 May 2011; revised 22 Jul 2011; accepted 1 Aug 2011; published 29 Aug 2011

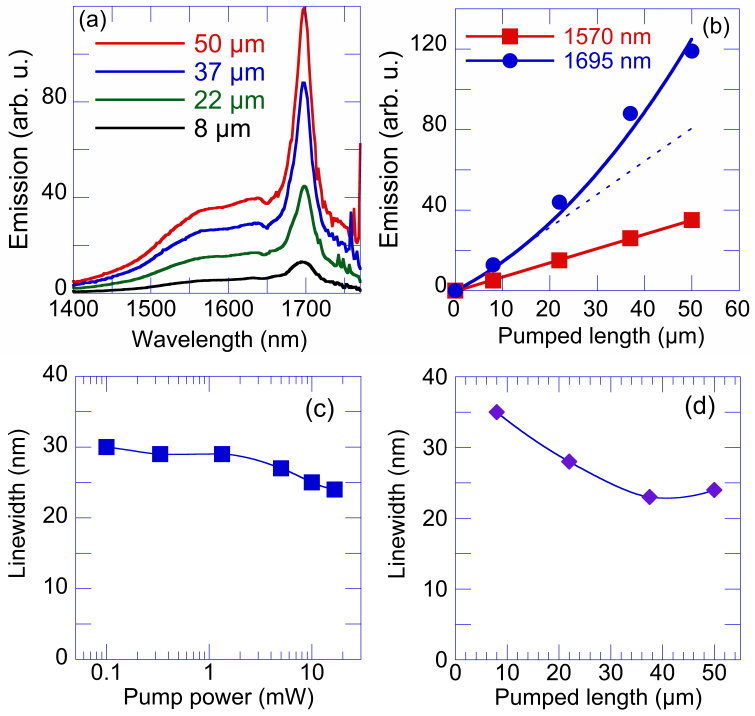

Fig. 4. (a) Room temperature photoluminescence of a single tensile-strained germanium wire as a function of the pumped length. The light is collected over the total wire length. (b) Peak amplitude of the emission at 1570 nm and 1695 nm. The red full line corresponds to a linear fit. The blue full line corresponds to a fit according to formula 1. The dashed line representing a linear dependence is shown for clarity. (c) Broadening (full width at half maximum) of the 1690 nm emission as a function of the incident pump power when the wire is fully illuminated. The full line is a guide to the eye. (d) Dependence of the broadening as a function of the pumping length for a fixed pump power. The full line is a guide to the eye.

is of the order of 1. In principle, we could estimate the optical gain from the amplitude variation of the broadening, following $\Delta\Gamma = \Delta\Gamma_0 \left[{}^{(G-1)}/_{(GLn(G))}\right]^{1/2}$ where $G = \exp(gl)$ [27]. An optical gain value g $\sim$ 200 cm^{-1} is deduced using this formula valid for Gaussian-broadened gain. However, as mentioned above, carrier distribution in direct and reciprocal space, inhomogeneous strain field, light propagation, self-absorption and the collection geometry should be taken into account for an accurate description of the linewidth reduction vs. gain and this modeling is beyond the scope of this article. We note that the self-absorption contributes to a reduced broadening of the room temperature spontaneous emission since the absorption is large at high energy. As the pumping intensity is increased, the bleaching of the absorption should first contribute to a decrease of self-absorption, i.e. an increase of the broadening, in particular if the bleaching of the absorption occurs on a large spectral range. When the absorption turns into gain, the linewidth starts to be reduced because of the amplification factor. The key feature reported in Fig. 4(c) is that the decreased broadening is an expected signature of optical gain. We have also investigated the broadening as a function of the pumping length for a fixed pump power. The result is shown in Fig. 4(d). A decrease of the broadening from 36 to 25 nm is

#147489 - $15.00 USD Received 12 May 2011; revised 22 Jul 2011; accepted 1 Aug 2011; published 29 Aug 2011

also observed when the pumping length is increased. This dependence corresponds also to the expected behavior when optical gain is present.

4. Conclusion

We have introduced a new method to impose a tensile stress on germanium and succesfully fabricated tensile-strained germanium photonic wires using Si_3N_4 straining layers. The tensile-strained layer exhibits a room temperature luminescence shifted by more than 120 nm from the bulk germanium. Optical gain has been evidenced at room temperature under cw optical pumping through the variable strip length method and the decrease of the broadening as the pump intensity or pumping length are increased. The observation of optical gain is a direct consequence of the applied tensile strain. The demonstration of optically active tensile-strained germanium wires opens new perspectives for the integration of compact optical sources on silicon and the study of novel nanoscale photonic elements [28, 29], similarly to the studies performed on nanowire lasers [30–32].

Acknowledgments

This work was partly supported by the French Ministry of Industry under Nano2012 convention and by RTRA “Triangle de la Physique”. We thank Daniel Bensahel from STMicroelectronics for his continuous support.

#147489 - $15.00 USD Received 12 May 2011; revised 22 Jul 2011; accepted 1 Aug 2011; published 29 Aug 2011